Analysis of Single Alzheimer Solid Plaque Cores by Laser Capture Microscopy and Nanoelectrospray/Tandem Mass Spectrometry

Linda Söderberg,[‡] Nenad Bogdanovic,[‡] Birgitta Axelsson,[§] Bengt Winblad,[‡] Jan Näslund,[‡] and Lars O. Tjernberg*[,‡]

Karolinska Institutet and Dainippon Sumitomo Pharma Alzheimer Center (KASPAC), Neurotec, Novum, and Department of Laboratory Medicine, Huddinge University Hospital, SE-141 57 Huddinge, Sweden

Received February 16, 2006; Revised Manuscript Received June 19, 2006

ABSTRACT: Aggregation of the 40−42 residue amyloid β-peptide (Aβ) into amyloid plaques is a central event in Alzheimer's disease (AD) pathogenesis. Many proteins have by immunohistochemical techniques been shown to codeposit with Aβ in AD plaques. It is possible that some of these could seed Aβ aggregation and therefore be found in the actual core of the plaque. Here, we present a highly sensitive method for unbiased biochemical analysis of plaque cores. A mild purification protocol based on centrifugation and filtration was used to purify intact plaque cores from human AD brain. The purified plaques were dispensed on a glass slide and viewed in a laser capture microscope, and plaque cores were catapulted into a tube cap by a laser beam. After dissolution in formic acid, plaques were digested and analyzed by liquid chromatography coupled online to electrospray/tandem mass spectrometry. One single plaque was found to be sufficient for positive identification of the main amyloid component. Remarkably, Aβ was the only protein identified when 200 plaques were isolated and analyzed with the present method. Thus, it is possible that no proteins copolymerize with Aβ in the plaque cores and that Aβ alone is sufficient for formation of plaque cores. In support of this notion, core-like structures were observed after incubation of synthetic Aβ for 2 weeks. We suggest that the method described here could be used for the general analysis of amyloid aggregates and inclusion bodies found in other neurodegenerative disorders and that plaque cores in AD brain are molecularly homogeneous structures.

The aggregation of proteins into insoluble fibrillar deposits, amyloid plaques, is an important pathogenic event in several different diseases (*1*). Alzheimer's disease (AD)[1] is characterized by the occurrence of plaques where the amyloid β-peptide (Aβ) is the main component (*2*). The 40−42 residue Aβ peptide is derived from the β-amyloid precursor protein (β-APP) through sequential proteolytic processing by the β- and γ-secretase enzymes (*3*). Aβ deposition in AD brain tissue results in the formation of morphologically distinct categories of plaques that to a varying degree provoke the occurrence of neurofibrillary tangles, the other major neuropathological lesion in AD. Among these are the cored, diffuse, and cotton wool-like plaques. The cored plaques are characterized by the maltese cross-like appearance of the plaque core after staining with the histological dye Congo red, whereas the latter two categories appear to be devoid of a core. Immunohistochemical studies have shown that all plaque types are positive for the Aβ40 and Aβ42 peptides but that the relative abundance of these species may vary between plaques (*4*). For instance, it has been hypothesized that peptides ending at Ala-42 are the main constituents of diffuse plaques and that these are the earliest lesions seen in AD brain (*5*). Cotton wool-like plaques, which were recently shown to be associated with rare forms of AD, are also predominantly Aβ42-positive (*6*). In addition, various plaque types may also be immunohistochemically distinguished by their relative content of amino-terminally truncated and posttranslationally modified Aβ peptides (*7*, *8*). Plaques are notoriously difficult structures to isolate and biochemically characterize; however, seminal work provided by Roher et al. (*9*, *10*) and others (*2*, *11*) is consistent with the immunohistochemical findings described above. Notably, a very recent study showed that amino-terminally truncated Aβ species are the main constituents of cotton wool-like plaques (*12*), although the role of these and other modified Aβ peptides in AD pathogenesis remains to be determined.

Many studies have shown that Aβ becomes neurotoxic upon aggregation (reviewed in ref *13*). Discrete intermediate oligomeric forms of Aβ can be detected during the aggregation process (*14*, *15*), and it is not fully known whether the mature fibrils, the intermediate protofibrils, or smaller diffusible aggregates mediate the toxicity (*16*, *17*). In addition, where and how the aggregation process is initiated is also unresolved (*18*). The concentration of Aβ in cerebrospinal fluid (CSF) and plasma is lower than the concentration required for in vitro aggregation of synthetic peptide (*19*). It is possible that aggregation in vivo is induced by high local concentrations of Aβ, metal ions, low pH, or pathological chaperones (*20*). In the latter case, it is hypothesized that the pathological chaperone protein interacts

* Corresponding author. Tel: 46 8 585 83620. Fax: 46 8 585 83610. E-mail: lars.tjernberg@ki.se.

[‡] Karolinska Institutet and Dainippon Sumitomo Pharma Alzheimer Center.

[§] Huddinge University Hospital.

[1] Abbreviations: Aβ, amyloid β-peptide; AD, Alzheimer's disease; HPLC, high-performance liquid chromatography; MS, mass spectrometry; MS/MS, tandem mass spectrometry; SDS, sodium dodecyl sulfate; TBS, Tris-buffered saline.

10.1021/bi060331+ CCC: $33.50
Published on Web 07/21/2006

with Aβ and induces aggregation. If a pathological chaperone binds to Aβ and initiates the aggregation, it may be codeposited with Aβ in the plaque core. Identifying these proteins and preventing them from interacting with Aβ could thus be a possible therapeutic approach for prevention and treatment of AD. Many proteins have been suggested to be associated with Aβ in amyloid plaques (*21*). Although most of these proteins appear to surround the plaque core, some could be directly involved in the aggregation process. For instance, α_1-antichymotrypsin (ACT) and apolipoprotein E (ApoE) affect Aβ aggregation and plaque density in mouse models (*22*−*24*). Interestingly, there is also a strong genetic linkage between one ApoE isoform, ApoE4, and AD (*25*). Other proteins, such as serum amyloid component P (SAP), seem to impede plaque turnover without being directly involved in the initial aggregation events (*26*, *27*).

It is worth noting that the majority of the plaque-associated proteins have been observed exclusively with immunochemical methods, and biochemical detail is lacking. Saitoh and co-workers (*28*) reported the first biochemical evidence suggesting the presence of a peptide other than Aβ in purified plaques. The peptide was initially termed NAC (non-Aβ component of AD amyloid) and was later found to be identical to a fragment of the presynaptic protein α-synuclein (*29*). α-Synuclein is the main component of Lewy bodies, aggregate inclusions found in many neurodegenerative diseases, e.g., AD, Parkinson's disease, and dementia with Lewy bodies. The colocalization of α-synuclein with Aβ in AD amyloid plaques has in subsequent studies been questioned (*30*, *31*). To discriminate between colocalization and localization in spatially separate aggregates, the ideal regime would be to analyze single aggregates. Technical limitations have thus far precluded this type of analysis.

Laser pressure catapulting (LPC) is a recently developed technique that has been used in the isolation of single cells (*32*). Briefly, a microscope is equipped with a laser, a precision mechanical table, and a digital camera. The system is computer-controlled, and the sample is observed both through the microscope objective and on the computer screen. The sample is placed on a microscopy slide and inserted into the microscope. Cells or other material to be isolated are located and labeled on the computer screen with the cursor. The labeled material is automatically positioned above the laser, and the selected material is catapulted by laser pressure. LPC uses the extremely high energy levels generated at the point of laser focus. By delivering a pulse of laser energy just below the focal plane of the specimen, the energy pulse drives the specimen up and into a tube cap placed above the sample. The high precision allows isolation of components as small as 1 μm, and there is no mechanical contact with the sample during transfer. Sensitive methods are necessary for analysis of the minute amounts of material isolated by LPC. Fortunately, technical advancements in high-performance liquid chromatography (HPLC) and tandem mass spectrometry (MS/MS) enable reliable identification of peptides at the high attomole to low femtomole level. Recently, laser capture microdissection in combination with mass spectrometry was used for identifying plaque-associated proteins (*33*, *34*) and for quantification of Aβ in plaques.

In the present paper we focus on the plaque cores and report a highly selective and sensitive method for the isolation and analysis of these from human AD brain. To purify the plaque cores, we performed various centrifugation and filtration steps. To further purify the plaques cores and exclude contaminants, we used LPC. The purified plaques were dissolved, digested, and analyzed by nano-flow HPLC-MS/MS. The current approach resulted in the isolation of pure plaques and was also very sensitive: one single plaque was sufficient for unbiased identification of Aβ. Interestingly, even when a large amount of plaque cores were analyzed, no other proteins except for Aβ were observed. When synthetic Aβ was incubated in vitro, structures indistinguishable from plaque cores were formed. Thus, plaque cores may form from Aβ only.

Also amyloid structures morphologically different from plaque cores were isolated from AD brain, analyzed, and demonstrated to be composed of Aβ. We suggest that the approach described here also could be applied for biochemical analysis of amyloid deposits and aggregates found in other neurodegenerative diseases.

EXPERIMENTAL PROCEDURES

Post-Mortem Material. Brain tissue was obtained from an 83-year-old man suffering from clinical Alzheimer disease 8 years prior to death. The cause of death was a heart attack, and the autopsy was performed 13 h post-mortem according to the protocol used in Huddinge Brain Bank, Huddinge Hospital, Sweden. The neuropathological investigation definitively confirmed the clinical AD diagnosis. Abundant senile plaques (neuritic, cored, and diffuse) in cortex and tangle formation in hippocampus and cortex, as well as extensive cortical congophilic angiopathy, were found in the tissue blocks taken from frontal, parietal, temporal, and limbic areas. For the biochemical study, the frontal cortical tissue was frozen and further processed.

Preparation of Plaque Cores. Two grams of tissue in 7 mL of Tris-buffered saline (TBS), pH 7.4, supplemented with protease inhibitor cocktail (Roche Diagnostics) was homogenized in a Potter-Elvehjem pestle homogenizer. TBS was added to a final volume of 25 mL, and the sample was vortex mixed. The homogenate was centrifuged in a fixed angle rotor at 50000*g* for 30 min, and the pellet was triturated in 3 mL of TBS, diluted to 25 mL in TBS, and centrifuged again at 50000*g* for 30 min. The resulting pellet was triturated as above, layered on top of a 30% sucrose cushion, and centrifuged at 50000*g* in an SW 41 rotor (Beckman Instruments) for 1 h. The tube was cut with a tube slicer at five positions. The fractions were stained overnight with Congo red (50% saturated in TBS) and viewed under polarized light. The pellet was layered on top of a 60% sucrose cushion and centrifuged for 3 h at 166000*g* in a TLS-55 rotor (Beckman Instruments). The pellet was suspended in TBS and filtered through a 40 μm nylon mesh (Millipore) in a 25 mm syringe filter holder. The filter was washed twice with 1.5 mL of TBS. The filtrate was centrifuged at 16000*g* for 10 min. The resulting pellet was washed twice with 1% sodium dodecyl sulfate (SDS) in TBS and put on top of 12 mL of 10% sucrose in a 15 mL falcon tube and centrifuged for 30 min at 4000*g*. One milliliter fractions (13 in total) were aspirated and viewed under polarized light. The disk on top of the 60% sucrose cushion was filtered through a 40 μm nylon mesh and washed with 1% SDS in TBS, as described above.

Immunostaining. The pellet from the 60% sucrose centrifugation was immunostained on coated slides (Super Frost

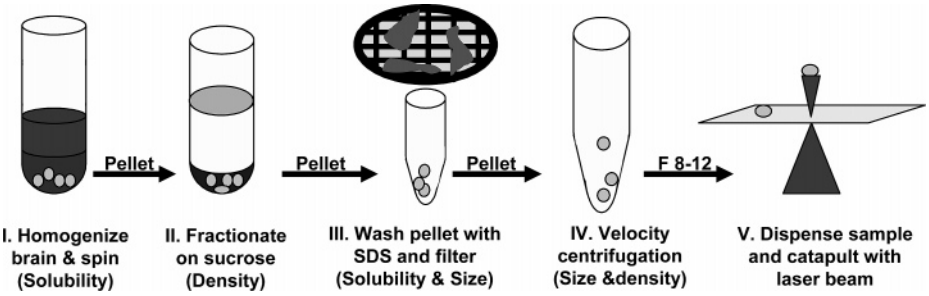

FIGURE 1: Scheme for purification of AD plaque cores. The pestle-homogenized material was centrifuged and washed repeatedly to remove soluble components (I). The pellet was placed on top of a 30% sucrose cushion and centrifuged at 50000*g* for 1 h. Congo red staining overnight showed that the plaque cores were present in the pellet. The pellet was placed on a 60% sucrose cushion and centrifuged at 166000*g* for 3 h (II). The disk (light gray) on top of the cushion contained some birefringent material but no plaque cores. Plaque cores and nuclei were found in the pellet, which was subsequently dissolved in TBS/1% SDS and filtered through a 40 μm nylon mesh (III). The filtrate was washed in TBS and centrifuged through 10% sucrose for 30 min at 4000*g* (IV). The pellet contained plaques and contaminating material. The fractions close to the pellet contained plaques and were less contaminated. These fractions were pooled and further purified by laser pressure catapulting (V).

Plus; Menzel-Gläser). Nonspecific sites were blocked with DAKO Protein Block (DAKO Corp.) for 30 min. The slides were incubated with monoclonal antibody 6E10 (Signet Laboratories Inc.) in 50 mM TBS at 4 °C overnight. Thereafter, the slides were incubated with secondary anti-mouse antibody followed by the avidin−biotin method using the Vectastatin ABC kit (Vector Laboratories). Finally, visualization was made by the use of a DAB (Sigma) dehydrated and mounted in DPX (BDH Laboratory Supplies). The specificity of the immunostaining procedure was determined by omitting the primary antibody.

Laser Capture Microscopy. The plaques from fractions 8−12 from the final centrifugation step described above were pooled, washed with H_2O, and dispensed on a microscope slide. The slide was air-dried and placed in the laser capture microscope (PALM Microlaser Technologies). The laser pulse energy was adjusted to 80 (where 100 is maximum), and the 40× objective was used. Plaque cores that were not close to any contaminating material were marked and captured (in a 0.6 mL tube cap with 30 μL of H_2O) by laser pressure catapulting. Birefringent aggregates from the disk at the top of the 60% cushion were localized in polarized light and isolated as described above.

Dissolution and Digestion of Purified Plaques. The purified plaques were dissolved in 90% formic acid (FA), 6 M guanidine thiocyanate (GdnSCN), or 0.1 M NaOH for 24 h with stirring. The aggregates from the disk were dissolved in 90% FA. The FA solution was frozen at −80 °C and lyophilized overnight, and 50 μL of 180 mM ammonium bicarbonate buffer (AmBic) containing 2 mM $CaCl_2$ and 0.5 μg trypsin (sequencing grade modified porcine trypsin; Promega Corp.) was added. The GdnSCN solution was diluted 10 times in the AmBic/$CaCl_2$/trypsin buffer. The pH of the NaOH solution was adjusted to 7 with HCl, and AmBic/$CaCl_2$/trypsin buffer was added. The samples were incubated at 37 °C overnight. The digested samples were desalted using ZipTips (Millipore) following the manufacturer's instructions. Bound peptides were eluted with 6 μL of 70% acetonitrile (ACN)/30% water/0.2% acetic acid. The eluent was evaporated in a vacuum centrifuge (Heto Lab Equipment A/S) for 5 min. About 1−2 μL of solvent was left after this procedure.

HPLC-MS/MS. The sample was injected onto a 0.1 × 150 mm C18 column (YMC Co., Ltd.) using a nano-LC injector (Valco Instruments) with a 1 μL loop. Peptides were eluted using a water/acetonitrile gradient supplemented with 0.2% FA: from 10% to 20% ACN in 10 min and 20−50% ACN in 60 min. The flow rate was 400 nL/min delivered by an Agilent 1100 nanopump (Agilent Technologies), and the column was coupled to an Agilent ion trap mass spectrometer (Agilent) fitted with a nanospray interface. Mass spectra were recorded from *m*/*z* 240 to *m*/*z* 2000, and the three most abundant peaks in each spectrum were automatically subjected to MS/MS analysis. The cycle time was 12 s.

Data Analysis. MS/MS spectra were analyzed using the NCBInr protein data bank and the Mascot software (Matrix Sciences). The scoring algorithm is probability based and takes into account the number of expected peaks that are found in the MS/MS spectrum in relation to the total number of peaks. Oxidation of methionine was included as a variable modification for samples dissolved in FA and guanidination for samples dissolved in GdnSCN. The search was restricted to fragments with at least one terminus corresponding to cleavage after lysine or arginine (trypsin or semitrypsin as the selected enzyme in MASCOT), and a maximum of one missed cleavage site was allowed.

Comparison of Detection Levels. Recombinant human ApoE3 (Sigma), ACT from human plasma (Sigma), and synthetic Aβ (Bachem) were diluted in AmBic/$CaCl_2$/trypsin buffer and digested with trypsin. In one case, Aβ was mixed with ApoE3 and ACT at a ratio of 60:1:1. The sample was incubated overnight at room temperature before digestion with trypsin.

Incubation of Synthetic Aβ. Synthetic Aβ1−40 (Bachem) was dissolved in DMSO (Sigma) to a concentration of 2 mg/mL, diluted to a final concentration of 25 μM in TBS, and incubated at room temperature (shaking 600 rpm) for 1 week. The samples were stained overnight with Congo red (50% saturated in TBS) and viewed under polarized light in a microscope.

RESULTS

Sample Preparation. Amyloid plaque cores were prepared from human brain using a protocol separating the brain material according to solubility, density, size, and sedimentation velocity (Figure 1). Homogenized human brain was fractionated and stained as described in Experimental Procedures. Birefringent spherical particles with a diameter

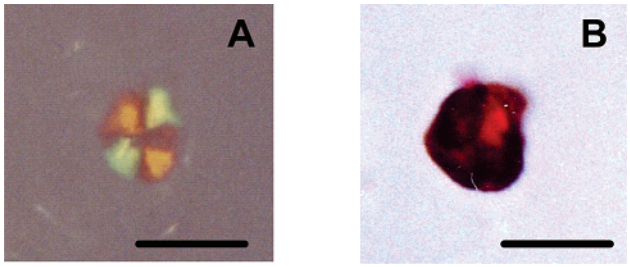

FIGURE 2: Purified plaque cores. (A) A purified AD plaque, 20 μm in diameter, stained with Congo red and viewed under polarized light at 400× magnification. Plaques were purified as described in Figure 1 and in Experimental Porcedures. (B) A plaque core stained with Congo red followed by immunostaining with monoclonal antibody 6E10 directed against Aβ. Note the brownish color of DAB-enhanced immunoreactivity as well as the brightness of Congo red staining under polarized filter. Bar = 20 μm.

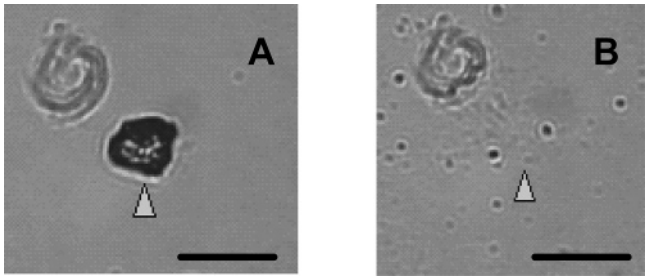

FIGURE 3: Laser pressure catapulting of purified plaques. (A) An aliquot of purified plaque cores was dispensed on a microscopy slide, and a selected plaque was marked on the computer screen. (B) The same slide after laser pressure catapulting of the marked plaque. The catapulted material was collected in a tube cap. Bar = 20 μm.

of 10−20 μm were exclusively found in the pellet fraction from the centrifugation in 30% sucrose (Figure 2A). These particles were also possible to stain using the Aβ antibody 6E10 (Figure 2B), and it was therefore concluded that they were authentic amyloid plaque cores. The pellet was mixed with 60% sucrose and centrifuged at 50000*g* for 3 h. The supernatant including a brown disk on top of the cushion, the sucrose fraction, and the pellet fraction were assayed for the presence of birefringent material. Most plaques were found in the pellet, which also contained cellular nuclei. The pellet was washed with 1% SDS and filtered through a 40 μm nylon mesh. By counting the Congo-stained plaques in the filtrate and on the filter disk, the recovery of plaques in the filtrate was estimated to be higher than 80%. The pellet was layered on top of a 10% sucrose cushion and centrifuged at 4000*g* for 30 min, whereafter 12 fractions were aspirated from the top and examined under polarized light. Fractions 8−12 and the pellet contained plaques, but the pellet contained more contaminating material than fractions 8−12. Therefore, fractions 8−12 were pooled and used for further studies.

Laser Capture Microscopy. As a final purification step, the purified plaque cores were isolated by laser capture microscopy. The pooled fractions were dispensed on a glass slide and viewed in the laser capture microscope. Red spherical particles with a diameter of 10−20 μm were selected and catapulted with a pulse from the laser (Figure 3). The catapulted material was collected in a test tube cap containing 30 μL of H_2O. Also, the material from the disk was viewed under polarized light, and birefringent aggregates were catapulted as described above (Figure 4).

The cap was attached to a test tube before centrifugation for 20 s. Formic acid (FA, 170 μL) and a small magnetic stirring bar were added to the tube. Other samples were treated with 6 M guanidine thiocyanate (GdnSCN) or 0.1 M NaOH. Samples were dissolved overnight at 25 °C with stirring. No plaques could be observed after treatment with either of the solvents. FA was the most efficient solvent as estimated by the Aβ^{17-28} fragment peak height (see below), followed by GdnSCN and NaOH. Samples dissolved in FA were lyophilized before digestion with trypsin. Trypsin is used for digestion since it generates fragments of suitable length and charge (usually 2+) for HPLC-MS/MS analysis. The GdnSCN-treated samples were diluted with digestion buffer, and the pH of the NaOH samples was adjusted before the addition of trypsin. Samples were digested overnight at 37 °C. ZipTips were used for concentration and desalting of the samples. The eluent was concentrated in a vacuum centrifuge to a final volume of 1−2 μL prior to injection into the HPLC-MS/MS system.

HPLC-MS/MS. One microliter of sample (corresponding to 50−100% of the total sample) was injected onto a 100 μm i.d. C18 column at a flow rate of 400 nL/min using an acetonitrile (ACN)/H_2O gradient for elution of the peptides. Not only does the final evaporation step concentrate the sample, it also lowers the ACN/H_2O ratio, making it possible to inject relatively large sample volumes without significant band broadening. The threshold for activation of MS/MS was set below the noise level in order to identify as many peptides as possible, and the three largest peaks in each MS scan were automatically subjected to MS/MS analysis. Thus, around 900 MS/MS spectra were recorded for each sample. The MS/MS spectra were searched against the NCBInr database using the MASCOT software. The charge of the mother ion was set to 2+ and 3+ (raw data were used in the database search since deconvolution of the spectra did not improve analysis). By using this approach Aβ^{17-28} was identified in a tryptic digest from one single catapulted plaque core (Figures 5A and 6). In addition to Aβ, different forms of human keratin (and porcine trypsin used for digestion) were identified (not shown). Injection of a digest from 20 catapulted plaque cores gave a proportionally higher signal-to-noise ratio (Figure 5B). Even when using this larger scale analysis, the peptides identified were exclusively derived from Aβ or from keratins. Keratin is a common contaminant, and the amount of keratin was not increased in the sample from 20 plaques compared to the single plaque analysis; therefore, we conclude that keratin is a contaminant and not a constituent of the plaque cores. The birefringent structures (Figure 4A,C) found in the disk on top of the 60% cushion were analyzed as above. Also in this case, Aβ^{17-28} as well as keratin was identified. The MS/MS from the structure in Figure 4C is shown in Figure 7. The quality of this spectrum is higher than the spectrum shown in Figure 6, possibly due to the larger amount of material injected (compare the size of the aggregates in Figures 3A and 4C).

The success of this protocol prompted us to perform a larger scale analysis to see whether any proteins other than Aβ were present in the plaque cores. Two hundred plaque cores were catapulted from one microscope slide and analyzed as above. Interestingly, no other proteins except

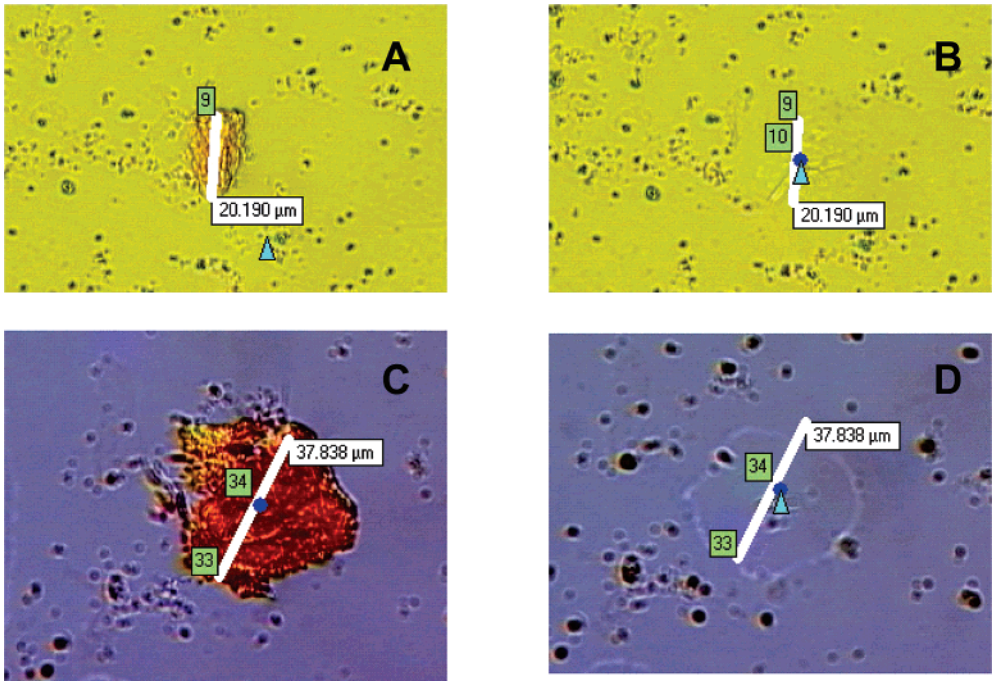

FIGURE 4: Laser pressure catapulting of amyloid aggregates. An aliquot of the disk from the top of a 60% sucrose cushion was dispensed on a microscopy slide and viewed under polarized light, and a large birefringent aggregate was labeled (A) and catapulted (B). The procedure was repeated with another birefringent aggregate (C, D).

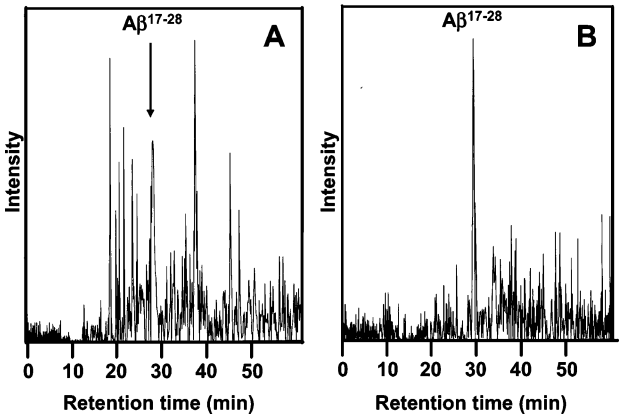

FIGURE 5: Extracted ion chromatograms from digests of (A) 1 and (B) 20 catapulted plaques. The plaques were dissolved in 90% FA overnight, lyophilized, and digested with trypsin. The sample was desalted and concentrated with ZipTips. One microliter of sample was injected into the LC-MS system. An ACN/H_2O gradient was used for elution of the peptides, and spectra were recorded from *m*/*z* 240 to *m*/*z* 1800. The chromatograms show *m*/*z* = 663.3, corresponding to $A\beta^{17-28} + 2H^+$.

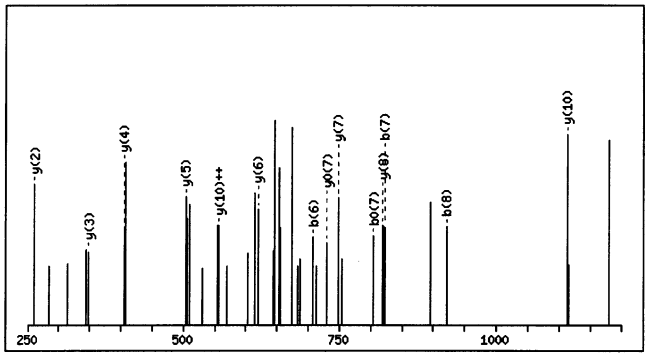

b	Mass	Sequence	y	Mass
1	114.09	L	12	
2	213.16	V	11	1212.59
3	360.23	F	10	**1113.52**
4	507.30	F	9	966.45
5	578.33	A	8	**819.38**
6	**707.38**	E	7	**748.35**
7	**822.40**	D	6	**619.31**
8	**921.47**	V	5	**504.28**
9	978.49	G	4	**405.21**
10	1065.53	S	3	**348.19**
11	1179.57	N	2	**261.16**
12		K	1	147.11

FIGURE 6: MS/MS spectrum of *m*/*z* = 663.3 eluting at 28.6 min in the chromatogram shown in Figure 5A. The three most abundant ions in each mass spectrum were automatically selected for MS/MS analysis. In total around 900 MS/MS spectra were generated from one sample. All MS/MS spectra were subjected to protein database search (NCBInr) using the Mascot software. The peptide yielding the present spectrum was identified as $A\beta^{17-28}$. The masses in bold indicate fragments found in the mass spectrum. The probability score, 45, was above the threshold for a significant hit.

for Aβ were identified. Thus, provided that the detection levels for potential plaque core proteins are similar as for Aβ, they would be present at a level less than 0.5%. We chose to compare the detection level of Aβ with two of the most well studied plaque-associated proteins, ACT and ApoE. The detection levels for Aβ and ApoE were similar, around 3 fmol, while ACT could be identified at a lower level (0.8 fmol) (data not shown). To mimic the conditions for plaque analysis, we incubated ACT and ApoE with an excess of Aβ (1:1:60) overnight before trypsin digestion. Also, in this case ACT could be detected at 0.8 fmol, while ApoE could be observed at 8 fmol (data not shown). Thus, at least the two most common plaque-associated proteins could be detected at similar levels as Aβ, and it is possible that Aβ could be the only protein in the plaque core. Therefore, we asked the question whether Aβ alone could form plaque core structures in the absence of pathological chaperones and tested this hypothesis in vitro.

Incubation of Synthetic Aβ. To investigate whether synthetic Aβ1−40 could form aggregates with morphology similar to the plaque cores isolated from brain, Aβ1−40 (25 μM) was incubated with stirring for 1 week. The Aβ solution

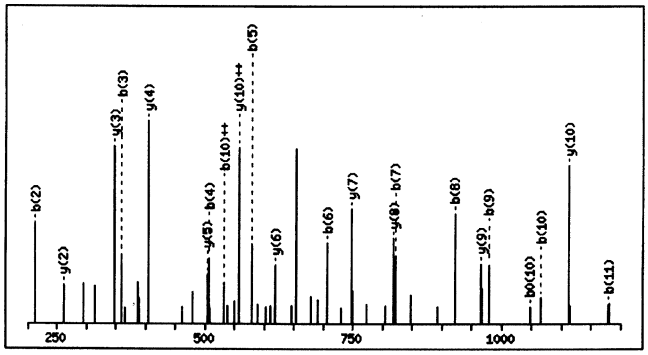

b	Mass	Sequence	y	Mass
1	114.09	L	12	
2	213.16	V	11	1212.59
3	360.23	F	10	1113.52
4	507.30	F	9	966.45
5	578.33	A	8	819.38
6	707.38	E	7	748.35
7	822.40	D	6	619.31
8	921.47	V	5	504.28
9	978.49	G	4	405.21
10	1065.53	S	3	348.19
11	1179.57	N	2	261.16
12		K	1	147.11

FIGURE 7: MS/MS spectrum generated from the single aggregate shown in Figure 4C. The catapulted aggregate was analyzed as described in Figure 6. The MS/MS from $m/z = 663.3$ is shown. The peptide yielding the present spectrum was identified as $A\beta^{17-28}$ (probability score = 90).

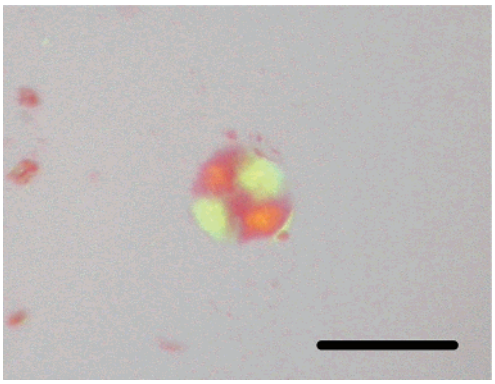

FIGURE 8: In vitro plaque core. Synthetic $A\beta 1-40$ (25 μM) was incubated in TBS, stained with Congo red, and viewed under polarized filter. Plaque cores around 10 μm in diameter was visualized. Bar = 15 μm.

was mixed with Congo red and viewed under polarized light. Birefringent spherical particles, similar to the plaque cores isolated from human brain, were visualized (Figure 8). The diameter of the core-like structures formed in vitro was slightly smaller than the cores isolated from human brain and were estimated to have a diameter of around 10 μm.

DISCUSSION

Here we show that it is possible to purify and analyze single plaque cores from human AD brain. The purification protocol is mild, and no proteases are used during the purification process; thus the risk of introducing protease-related artifacts is minimized. The final purification step, laser pressure catapulting, results in a virtually pure plaque preparation. A few very recent studies have also reported the use of the laser capture microdissection and catapulting technique to obtain more information on the biochemical makeup of AD plaques (*12*, *33*, *34*). In these studies, plaques were directly laser dissected from AD brain tissue sections. In principle, this experimental paradigm allows identification of proteins that are surrounding the plaque cores. In an extensive study, Liao and co-workers (*34*) have shown that many proteins of different nature and function can be identified in this way. However, careful interpretation and secondary analysis of the results are warranted, since many of the proteins may be components of the tissue surrounding the plaque, with little or no effect on the plaque genesis or turnover per se. Here we chose to focus on the cores of AD plaques and use laser catapulting as a final instead of a first purification step. The relatively uniform size and density of AD plaque cores allow for a stringent purification regimen and subsequent biochemical analysis of core protein components, while minimizing possible confounding results due to nonrelevant copurifying proteins. Further studies are required to determine whether the experimental protocol described here can be applied in the molecular analysis of diffuse and cotton wool-like AD plaques.

In our study, one single amyloid plaque core was sufficient for positive identification of $A\beta^{17-28}$, a tryptic fragment derived from Aβ. The present approach opens new possibilities for the analysis of amyloid deposits. Many previous studies on AD plaque biochemistry have depended on bulk analysis of large quantities of plaques (*11*, *35*, *36*). If plaque-associated proteins are found in such bulk analyses, it is not possible to discriminate between the following two possibilities: (i) the identified protein is present in all plaques, or (ii) the identified protein is present only in a subset of the plaques. As mentioned above, it can also be envisioned that proteins from the tissue surrounding the plaques copurify with plaques when purified in bulk and confound subsequent biochemical analysis. In this context it should be noted that it is possible to use the present method for the analysis of a large number of plaques in order to identify plaque components that are present at low levels. Assuming that the amount needed for identification of a potential plaque protein is the same as for Aβ, the analysis of 200 catapulted plaques as presented here would be sufficient for identification of a protein at the 0.5% (mol/mol of Aβ) level. We showed that the identification levels were similar for Aβ and ApoE and even lower for ACT. Thus, at least these two so-called plaque-associated proteins are not present in the cores at levels above 0.5%. There are, however, several possibilities for a protein to escape identification using the present purification protocol: (i) the recovery is much lower than for Aβ; (ii) the sequence is not present in the database used for the MS/MS search; or (iii) the putative protein has undergone modifications generating fragments undetectable in the database search. In exploratory experiments where we analyzed proteins in the less dense disk fraction, we found sequences corresponding to the canonical plaque-associated proteins ApoE and ACT and also the recently identified CLAC protein (*37*) (results not shown). It is therefore possible that these proteins are associated with plaques without being bona fide components of the plaque core. Tandem mass spectrometry allows identification of a protein based on the MS/MS spectrum from a single unique tryptic peptide. The lack of identified Aβ fragments other than $A\beta^{17-28}$ could be explained by their chromatographic or mass spectrometric properties, as for instance in the case of the extremely hydrophobic C-terminal fragments ($A\beta^{29-40}$ and

Aβ^{29-42}). Also, highly polar peptides such as Aβ^{1-5} and Aβ^{6-16} could be lost in the desalting procedure or result in low-quality MS/MS spectra. Accordingly, when synthetic Aβ^{1-42} was digested and analyzed using the same experimental approach as for plaque core-extracted Aβ, the Aβ^{17-28} fragment was conspicuously the most abundant fragment. The relative peak areas were found to be 10% for Aβ^{6-16}, 5% for Aβ^{29-42}, and 0.5% for Aβ^{1-5} (Aβ^{17-28} was set to 100%; results not shown). Moreover, deposited Aβ is a heterogeneous mixture of N-terminally truncated and sometimes modified variants, starting at residues ranging from 1 to 11. Thus, the concentration of a specific N-terminal species will be relatively low. Similar differences in response as described above will occur also for tryptic peptides generated from other proteins, and it is possible that in extreme cases none of the fragments would yield a high-quality spectrum.

The present study does not address the possible codeposition of nonprotein compounds known to affect Aβ aggregation in vitro, such as lipids, carbohydrates, or metal ions. Interestingly, a very recent study demonstrated that laser capture microdissection can be used to determine the presence of metal ions in plaque-like deposits in a mouse model of AD (*38*), thus opening avenues for future research aimed at probing the content of nonprotein components of AD plaques.

Studies using transgenic mice that overexpress either ApoE or ACT have demonstrated that both proteins affect Aβ deposition in vivo (*22*, *23*), although the mechanism underlying this phenomenon remains unknown. It has been speculated that a C-terminal fibril-forming fragment of ApoE can serve as a nidus for further Aβ aggregation (*39*). We could not detect proteins other than Aβ in AD plaque cores, indicating that Aβ alone can form these structures. This is supported by the finding that synthetic Aβ1−40 after incubation for a prolonged time in a physiological buffer can form maltese cross-like cores seemingly indistinguishable from the cores isolated from AD brain (cf. Figures 2A and 8). While additional studies are clearly needed, we hypothesize that the plaque-associated proteins play a more important role at a later stage in the plaque formation process, affecting turnover and clearance, rather than acting as pathological chaperones.

We suggest that the general outline of the present method could be used for detailed biochemical analysis of AD plaques and other protein aggregates, such as the inclusions seen in neurodegenerative tauopathies and Lewy body dementia.

ACKNOWLEDGMENT

We are grateful to Inga Volkmann for experienced supervision of the plaque microscopy work.

REFERENCES

1. Rochet, J. C., and Lansbury, P. T., Jr. (2000) Amyloid fibrillogenesis: themes and variations, *Curr. Opin. Struct. Biol. 10*, 60−68.
2. Masters, C. L., Simms, G., Weinman, N. A., Multhaup, G., McDonald, B. L., and Beyreuther, K. (1985) Amyloid plaque core protein in Alzheimer disease and Down syndrome, *Proc. Natl. Acad. Sci. U.S.A. 82*, 4245−4249.
3. Sambamurti, K., Greig, N. H., and Lahiri, D. K. (2002) Advances in the cellular and molecular biology of the β-amyloid protein in Alzheimer's disease, *Neuromol. Med. 1*, 1−31.
4. Selkoe, D. J. (2001) Alzheimer's disease: genes, proteins, and therapy, *Physiol. Rev. 81*, 741−766.
5. Iwatsubo, T., Odaka, A., Suzuki, N., Mizusawa, H., Nukina, N., and Ihara, Y. (1994) Visualization of Aβ42(43) and Aβ40 in senile plaques with end-specific Aβ monoclonals: evidence that an initially deposited species is Aβ42(43), *Neuron 13*, 45−53.
6. Crook, R., Verkkoniemi, A., Perez-Tur, J., Mehta, N., Baker, M., Houlden, H., Farrer, M., Hutton, M., Lincoln, S., Hardy, J., Gwinn, K., Somer, M., Paetau, A., Kalimo, H., Ylikoski, R., Poyhonen, M., Kucera, S., and Haltia, M. (1998) A variant of Alzheimer's disease with spastic paraparesis and unusual plaques due to deletion of exon 9 of presenilin 1, *Nat. Med. 4*, 452−455.
7. Saido, T. C., Iwatsubo, T., Mann, D. M., Shimada, H., Ihara, Y., and Kawashima, S. (1995) Dominant and differential deposition of distinct beta-amyloid peptide species, Aβ N3(pE), in senile plaques, *Neuron 14*, 457−466.
8. Iwatsubo, T., Saido, T. C., Mann, D. M., Lee, V. M., and Trojanowski, J. Q. (1996) Full-length amyloid-β (1−42(43)) and amino-terminally modified and truncated amyloid-β 42(43) deposit in diffuse plaques, *Am. J. Pathol. 149*, 1823−1830.
9. Roher, A. E., Lowenson, J. D., Clarke, S., Wolkow, C., Wang, R., Cotter, R. J., Reardon, I. M., Zurcher-Neely, H. A., Heinrikson, R. L., Ball, M. J., and Greenberg, B. D. (1993) Structural alterations in the peptide backbone of? β-amyloid core protein may account for its deposition and stability in Alzheimer's disease, *J. Biol. Chem. 268*, 3072−3083.
10. Roher, A. E., Lowenson, J. D., Clarke, S., Woods, A. S., Cotter, R. J., Gowing, E., and Ball, M. J. (1993) β-Amyloid-(1−42) is a major component of cerebrovascular amyloid deposits: implications for the pathology of Alzheimer disease, *Proc. Natl. Acad. Sci. U.S.A. 90*, 10836−10840.
11. Miller, D. L., Papayannopoulos, I. A., Styles, J., Bobin, S. A., Lin, Y. Y., Biemann, K., and Iqbal, K. (1993) Peptide compositions of the cerebrovascular and senile plaque core amyloid deposits of Alzheimer's disease, *Arch. Biochem. Biophys. 301*, 41−52.
12. Miravalle, L., Calero, M., Takao, M., Roher, A. E., Ghetti, B., and Vidal, R. (2005) Amino-terminally truncated Aβ peptide species are the main component of cotton wool plaques, *Biochemistry 44*, 10810−10821.
13. Sayre, L. M., Zagorski, M. G., Surewicz, W. K., Krafft, G. A., and Perry, G. (1997) Mechanisms of neurotoxicity associated with amyloid beta deposition and the role of free radicals in the pathogenesis of Alzheimer's disease: a critical appraisal, *Chem. Res. Toxicol. 10*, 518−526.
14. Ward, R. V., Jennings, K. H., Jepras, R., Neville, W., Owen, D. E., Hawkins, J., Christie, G., Davis, J. B., George, A., Karran, E. H., and Howlett, D. R. (2000) Fractionation and characterization of oligomeric, protofibrillar and fibrillar forms of β-amyloid peptide, *Biochem. J. 348* (Part 1), 137−144.
15. Bitan, G., Lomakin, A., and Teplow, D. B. (2001) Amyloid β-protein oligomerization: prenucleation interactions revealed by photo-induced cross-linking of unmodified proteins, *J. Biol. Chem. 276*, 35176−35184.
16. Lorenzo, A., and Yankner, B. A. (1994) β-Amyloid neurotoxicity requires fibril formation and is inhibited by congo red, *Proc. Natl. Acad. Sci. U.S.A. 91*, 12243−12247.
17. Walsh, D. M., Klyubin, I., Fadeeva, J. V., Rowan, M. J., and Selkoe, D. J. (2002) Amyloid-β oligomers: their production, toxicity and therapeutic inhibition, *Biochem. Soc. Trans. 30*, 552−557.
18. Glabe, C. (2001) Intracellular mechanisms of amyloid accumulation and pathogenesis in Alzheimer's disease, *J. Mol. Neurosci. 17*, 137−145.
19. Vanderstichele, H., Van Kerschaver, E., Hesse, C., Davidsson, P., Buyse, M. A., Andreasen, N., Minthon, L., Wallin, A., Blennow, K., and Vanmechelen, E. (2000) Standardization of measurement of β-amyloid(1−42) in cerebrospinal fluid and plasma, *Amyloid 7*, 245−258.
20. McLaurin, J., Yang, D., Yip, C. M., and Fraser, P. E. (2000) Review: modulating factors in amyloid-β fibril formation, *J. Struct. Biol. 130*, 259−270.
21. Atwood, C. S., Martins, R. N., Smith, M. A., and Perry, G. (2002) Senile plaque composition and posttranslational modification of amyloid-β peptide and associated proteins, *Peptides 23*, 1343−1350.
22. Nilsson, L. N., Bales, K. R., DiCarlo, G., Gordon, M. N., Morgan, D., Paul, S. M., and Potter, H. (2001) Alpha-1-antichymotrypsin

promotes β-sheet amyloid plaque deposition in a transgenic mouse model of Alzheimer's disease, *J. Neurosci. 21*, 1444−1451.
23. Holtzman, D. M., Fagan, A. M., Mackey, B., Tenkova, T., Sartorius, L., Paul, S. M., Bales, K., Ashe, K. H., Irizarry, M. C., and Hyman, B. T. (2000) Apolipoprotein E facilitates neuritic and cerebrovascular plaque formation in an Alzheimer's disease model, *Ann. Neurol. 47*, 739−747.
24. Carter, D. B., Dunn, E., McKinley, D. D., Stratman, N. C., Boyle, T. P., Kuiper, S. L., Oostveen, J. A., Weaver, R. J., Boller, J. A., and Gurney, M. E. (2001) Human apolipoprotein E4 accelerates β-amyloid deposition in APPsw transgenic mouse brain, *Ann. Neurol. 50*, 468−475.
25. Saunders, A. M. (2000) Apolipoprotein E and Alzheimer disease: an update on genetic and functional analyses, *J. Neuropathol. Exp. Neurol. 59*, 751−758.
26. Tennent, G. A., Lovat, L. B., and Pepys, M. B. (1995) Serum amyloid P component prevents proteolysis of the amyloid fibrils of Alzheimer disease and systemic amyloidosis, *Proc. Natl. Acad. Sci. U.S.A. 92*, 4299−4303.
27. Pepys, M. B., Herbert, J., Hutchinson, W. L., Tennent, G. A., Lachmann, H. J., Gallimore, J. R., Lovat, L. B., Bartfai, T., Alanine, A., Hertel, C., Hoffmann, T., Jakob-Roetne, R., Norcross, R. D., Kemp, J. A., Yamamura, K., Suzuki, M., Taylor, G. W., Murray, S., Thompson, D., Purvis, A., Kolstoe, S., Wood, S. P., and Hawkins, P. N. (2002) Targeted pharmacological depletion of serum amyloid P component for treatment of human amyloidosis, *Nature 417*, 254−259.
28. Ueda, K., Fukushima, H., Masliah, E., Xia, Y., Iwai, A., Yoshimoto, M., Otero, D. A., Kondo, J., Ihara, Y., and Saitoh, T. (1993) Molecular cloning of cDNA encoding an unrecognized component of amyloid in Alzheimer disease, *Proc. Natl. Acad. Sci. U.S.A. 90*, 11282−11286.
29. Iwai, A., Masliah, E., Yoshimoto, M., Ge, N., Flanagan, L., de Silva, H. A., Kittel, A., and Saitoh, T. (1995) The precursor protein of non-Aβ component of Alzheimer's disease amyloid is a presynaptic protein of the central nervous system, *Neuron 14*, 467−475.
30. Wirths, O., and Bayer, T. A. (2003) Alpha-synuclein, Aβ and Alzheimer's disease, *Prog. Neuropsychopharmacol. Biol. Psychiatry 27*, 103−108.
31. Wirths, O., Weickert, S., Majtenyi, K., Havas, L., Kahle, P. J., Okochi, M., Haass, C., Multhaup, G., Beyreuther, K., and Bayer, T. A. (2000) Lewy body variant of Alzheimer's disease: alpha-synuclein in dystrophic neurites of Aβ plaques, *Neuroreport 11*, 3737−3741.
32. Schutze, K., Posl, H., and Lahr, G. (1998) Laser micromanipulation systems as universal tools in cellular and molecular biology and in medicine, *Cell. Mol. Biol. (Noisy-le-grand) 44*, 735−746.
33. Rufenacht, P., Guntert, A., Bohrmann, B., Ducret, A., and Dobeli, H. (2005) Quantification of the Aβ peptide in Alzheimer's plaques by laser dissection microscopy with mass spectrometry, *J. Mass Spectrom. 40*, 193−201.
34. Liao, L., Cheng, D., Wang, J., Duong, D. M., Losik, T. G., Gearing, M., Rees, H. D., Lah, J. J., Levey, A. I., and Peng, J. (2004) Preoteomic characterization of postmortem amyloid amyloid plaques by laser capture microdissection, *J. Biol. Chem. 279*, 37061−37068.
35. Wong, C. W., Quaranta, V., and Glenner, G. G. (1985) Neuritic plaques and cerebrovascular amyloid in Alzheimer disease are antigenically related, *Proc. Natl. Acad. Sci. U.S.A. 82*, 8729−8732.
36. Selkoe, D. J., Abraham, C. R., Podlisny, M. B., and Duffy, L. K. (1986) Isolation of low-molecular-weight proteins from amyloid plaque fibers in Alzheimer's disease, *J. Neurochem. 46*, 1820−1834.
37. Hashimoto, T., Wakabayashi, T., Watanabe, A., Kowa, H., Hosoda, R., Nakamura, A., Kanazawa, I., Arai, T., Takio, K., Mann, D. M., and Iwatsubo, T. (2002) CLAC: a novel Alzheimer amyloid plaque component derived from a transmembrane precursor, CLAC-P/collagen type XXV, *EMBO J. 21*, 1524−1534.
38. Hutchinson, R. W., Cox, A. G., McLeod, C. W., Marshall, P. S., Harper, A., Dawson, E. L., and Howlett, D. R. (2005) Imaging and spatial distribution of β-amyloid peptide and metal ions in Alzheimer's plaques by laser-ablation-inductively coupled plasma-mass spectrometry, *Anal. Biochem. 346*, 225−233.
39. Wisniewski, T., Lalowski, M., Golabek, A., Vogel, T., and Frangione, B. (1995) Is Alzheimer's disease an apolipoprotein E amyloidosis?, *Lancet 345*, 956−958.

BI060331+